

Mutual shielding of closely spaced dust particles in low pressure plasmas

Seung J. Choi^{a)} and Mark J. Kushner^{b)}

University of Illinois, Department of Electrical and Computer Engineering, 1406 West Green Street, Urbana, Illinois 61801

(Received 23 September 1993; accepted for publication 10 December 1993)

The transport of particles ("dust") in low pressure electrical glow discharges is of interest as a result of their role in contaminating wafers during plasma etching and deposition of semiconductors. Particles (10s nm to many micrometers) negatively charge in glow discharges and, to first order, appear to be massively large negative ions around which sheaths develop. The electrical and fluid forces acting on dust particles in plasma processing discharges may cause the interparticle spacing to be less than the shielding distance around particles. The mutual shielding of dust particles is therefore of interest. In this article, we report on results from a pseudoparticle-in-cell simulation of the mutual shielding of two adjacent dust particles. Results will be discussed for charge, potential, and electrostatic forces on dust particles as a function of particle size and separation distance between two particles. We found that two closely spaced particles not only shield each other but can shadow their partner, thereby resulting in asymmetric charging of otherwise identical particles.

I. INTRODUCTION

Particulates ("dust" particles) are common contaminants in low pressure (< 100 s mTorr), partially ionized (electron density 10^9 – 10^{11} cm⁻³) plasma processing electrical glow discharges for semiconductor etching and deposition. Many experimental and theoretical investigations have recently been conducted to determine the manner in which particles transport in plasma processing reactors; and to quantify the electrical and mechanical forces on dust particles.^{1–18} The general findings are that dust particles negatively charge in low temperature plasmas, and particles of a few micrometers in size have 100s to 1000s of elementary charges. The negative charge balances the flux of electrons and ions to the particle surface. This generates floating potentials of 1.5 – $3T_e$, where the electron temperature T_e in typical discharges is 2–5 eV.¹⁹ The plasma shielding distance around particles is best characterized by a linearized Debye length, λ_D , having typical values of many to 10s of micrometers.^{1,2} Therefore, if the local densities of dust particle densities are $\ll 10^6$ cm⁻³, they can be analyzed as isolated entities.

Dust particles generally accumulate in radio frequency (rf) discharges in specific regions of the plasma. Roth and Spears first used laser light scattering to observe that particles accumulate near the bulk plasma-sheath boundary,³ as later confirmed by Selwyn *et al.*,^{4–6} Jellum *et al.*,^{7–9} and Watanabe *et al.*^{10,11} Large particles (> 0.1 μ m) accumulate near the sheath edge, while small particles accumulate in the center of the discharge at the location of the maximum in the plasma potential. Selwyn *et al.*⁵ and Carlisle *et al.*¹² also observed that particles accumulated at the sheath-plasma boundary in rings around semi-

conductor wafers and domes above the wafers in etching rf discharges.

Sommerer *et al.*¹³ and Barnes *et al.*¹⁴ have proposed that transport of small particles (when gravity and thermophoresis are not important) is dominated by two forces; electrostatic and viscous ion drag. The former force accelerates negatively charged particles towards the center of electropositive plasmas or towards local maxima in the plasma potential. The latter force accelerates particles in the direction of net ion flux, which is generally towards the boundaries of the plasma. (The ion drag force results from open orbits of positive ions around the dust particle which transfers momentum to the particle in the direction of the net ion flux.) For large particles in moderate density plasmas (10^9 – 10^{10} cm⁻³), these forces balance near the sheath edge where the large electric fields in the sheath push the particle towards the center of the plasma, while ion drag pushes the particle towards the boundary. Recent electric probe measurements of the plasma potential in rf discharges have also revealed that particles are commonly found in positive potential traps (perhaps as large as 7 V).¹⁵

Laser light scattering and visual observations of the accumulation of dust particles have revealed regions of dense accumulation of particles where the separation between particles is commensurate with the shielding distances. For example, Boufendi *et al.* have observed dust particles (100s nm in size) at densities exceeding 10^8 cm⁻³ in Ar/SiH₄ plasmas.¹⁶ The Coulomb coupling parameter for these conditions is $\Gamma \approx 10$. Their observations of dust particle motion are consistent with the dusty plasma acting as a Coulomb liquid.

Our interest in this work is the interaction of two closely spaced dust particles in an otherwise pristine plasma. Dust particles can obtain kinetic energies of 100s eV to many keV by acceleration from ion and fluid drag

^{a)}Present address: Sandia National Laboratories, Albuquerque, NM 87185.

^{b)}Author to whom correspondence should be addressed.

forces. These energies greatly exceed the interparticle potentials. Therefore, even highly charged dust particles can approach and collide with each other. Collisions of this sort result from dust particles originating from different locations in the plasma, and therefore may have differential velocities of the required magnitudes to overcome the Coulomb repulsion. For example, stressed films on the wall of plasma etching reactors can emit particles into the plasma.²⁰ Kilgore *et al.*²¹ have shown that these particles will be accelerated to 100s keV in ECR reactors, and therefore can collide with quasistationary dust particles suspended at sheath edges.

To investigate conditions where dust particles are within each other's shielding volumes we have developed a pseudoparticle-in-cell computer simulation of the charging and shielding of adjacent dust particles in low temperature plasmas. (To avoid confusion, the computational electron and ion particles used in the simulation will be called pseudoparticles. The dust particulates will be called dust particles.) In this model, electron and ion energy distribution functions and densities are obtained in the vicinity of one or more dust particles while solving Poisson's equations for the electric field. The results of the model provide the shielding distances, the effective momentum transfer cross sections of the dust particle, and the magnitudes of the ion drag and electrostatic forces. We found that closely spaced particles do mutually shield each other. The presence of an adjacent particle reduces the charge requirement on the first particle by deflecting and intercepting incident electrons. Particles shadowed (with respect to the net electron flux) by adjacent particles also charge to less negative values.

The model is described in Sec. II, followed by a discussion of our results in Sec. III. Our concluding remarks are in Sec. IV.

II. DESCRIPTION OF THE MODEL

The model we have used in this study is based on a previously described simulation for the shielding of single dust particles.^{2,16} That model will be briefly described, followed by a discussion of modifications to the model to address multiple dust particles.

Before executing the pseudoparticle-in-cell simulation (PICS), Monte Carlo simulations (MCS) of both the electron and ion swarms are performed using a specified and spatially uniform E/N (electric field/gas number density). The purpose of performing the MCS is to obtain the quasi-steady state electron energy distribution and ion energy distribution for use as initial conditions in the PICS. The details of the MCS are described in Ref. 22. All pertinent elastic and inelastic collisions of electrons with the neutral gas and ions are included in the MCS. In this investigation we studied contaminated argon plasmas, and the sources of our electron impact cross sections are listed in Ref. 22. The collisions included in the MCS for ions are elastic (ion-neutral) and charge exchange (ion-neutral), with cross sections derived from swarm data,^{23,24} and elastic Coulomb (ion-ion).

After the initial electron and ion energy distributions are determined, a dust particle is introduced into the center of the computational volume. The PICS is then performed while including all of the collision processes described above. This portion of the model differs from the MCS in that now the self-consistent electric field in the vicinity of the dust particle is calculated by solving Poisson's equation while the equations of motion of the pseudoparticles are advanced. When investigating single particles, Poisson's equation is solved in spherical coordinates in a subvolume centered on the dust particle. The spherical subvolume is centered in a larger rectangular space to which periodic boundary conditions are applied. When solving Poisson's equation, the net charge density in the plasma and on the surface of the dust particle are accounted for. The surface charge density provides a boundary condition in the form of the electric field at the surface.

Pseudoparticles striking the dust particle are assumed to be collected with unity efficiency. The specified externally applied E/N (to heat the electron swarm) defines the net potential drop across the computational volume, which is always small compared to the floating potential of the dust particle. The boundary condition on the boundary of the computational volume is then $-(\nabla\phi/N) \cdot \hat{z} = E/N$. The mesh spacing and time steps of the pseudoparticles were chosen to insure correct representation of pseudoparticle trajectories at all pertinent impact parameters. The collected charge density is usually averaged over the surface of the dust particle. We usually begin the PICS with an estimated charge Q on the particle, and the PICS is executed to obtain dQ/dt . Based on the sign of dQ/dt , the PICS is repeated with different values of Q to search for the value of Q that yields $dQ/dt=0$.

To simulate multiple dust particles, the following enhancements to the model were made. We first modified the simulation to have a two-dimensional rectilinear coordinate system. The locations, shapes, and sizes of an arbitrary number of dust particles were specified by identifying each cell of the computational mesh as being either "plasma" or "dust." Computationally, this was accomplished by including a volumetric charge density at each cell center (for contributions from the plasma) and surface charge densities at the boundaries of all cells (for contributions from the surface of the dust). A stencil identifying each cell center and cell boundary as being either "plasma" or "dust" was then employed to both include the appropriate charge density in solution of Poisson's equation, and to increment contributions from the pseudoparticles (either volumetric density or flux to the surface) to the charge densities. Poisson's equation was then solved using the method of successive overrelaxation.

The method just described was computationally expedient. However, as a consequence of using a rectilinear coordinate system, the surface-to-volume ratio of the dust particles was unrealistically large. We found that for our typical conditions, well over half of the negative charge eventually resided on the dust particles. Also, the orbital dynamics of the pseudoparticles (which are computed in three spatial dimensions) were not well represented since

the dust particles appeared two dimensional. We therefore modified the model to use cylindrical coordinates that allow the particles to approximately retain the surface-to-volume ratios of spherical particles, and allows three-dimensional orbital dynamics. Using this option, the dust particles are restricted to being a string of particles aligned on the central axis. However, using the stenciling convention described above, the dust particles can have any shape which can be represented by a collection of cylinders or washer shaped disks.

From previous experience, we learned that to avoid numerical biasing each pseudoparticle should represent a single electron or ion, and the mesh spacing near the dust particle should not exceed a few tenths of the particle dimension.^{2,19} This results in using a large number of pseudoparticles (25 000–100 000) and a computational mesh for solution of Poisson's equation which is $100s \times 100s$. To minimize computer time, we nested the cylindrical subvolume upon which Poisson's equation is solved inside a larger rectilinear region to which periodic boundary conditions are applied. The boundary condition for Poisson's equation at the edge of the cylindrical subvolume is given by the potential wrought by the externally applied electric field. When outside the subvolume, pseudoparticles are moved with time steps usually given by the time between solution of Poisson's equation. In the cylindrical subvolume, there is considerable subcyclng of electron and ion pseudoparticles to both resolve the local electric field and to take advantage of the different time scales afforded by the heavy ions and light electrons.

III. MUTUAL SHIELDING OF DUST PARTICLES

The model was used to investigate the mutual shielding of two closely spaced dust particles. The model was parametrized over the separation distance of the dust particles and the particle size. Quasi-steady state electrical potential profiles around two dust particles that are good conductors are shown in Fig. 1 for two different (face-to-face) particle separations, 2.2 and $7.3 \mu\text{m}$. The gas pressure is 0.2 Torr of Ar, the bulk plasma density is $3 \times 10^{11} \text{ cm}^{-3}$, and the applied E/N is $30 \times 10^{-17} \text{ V cm}^2$, generating an electron temperature of 3.9 eV far from the dust particle. These conditions were chosen to approximate those of high plasma density etching reactors.²⁵ The electric field is aligned along the z axis so that electrons drift from negative to positive z . Two identical cylindrical dust particles of $1 \mu\text{m}$ diameter and a height of $0.9 \mu\text{m}$ are used. The potential of the isolated particles is $\approx -14.2 \text{ V}$. The linearized Debye length is $\lambda_L = 7.3 \mu\text{m}$.²⁶

With the smaller spacing shown in Fig. 1(a), the shielding volumes of the two dust particles overlap to $\approx -7 \text{ V}$. At distances exceeding $3\text{--}4 \mu\text{m}$, the particles appear to be a single potential source. When two dust particles are separated by at least a few λ_L , as shown in Fig. 1(b), they appear like individual particles. Since the shielding volumes of adjacent dust particles overlap, the effective momentum transfer cross section for ions or electrons colliding with the particles is less than the sum of individual dust particle cross sections obtained at large separations.

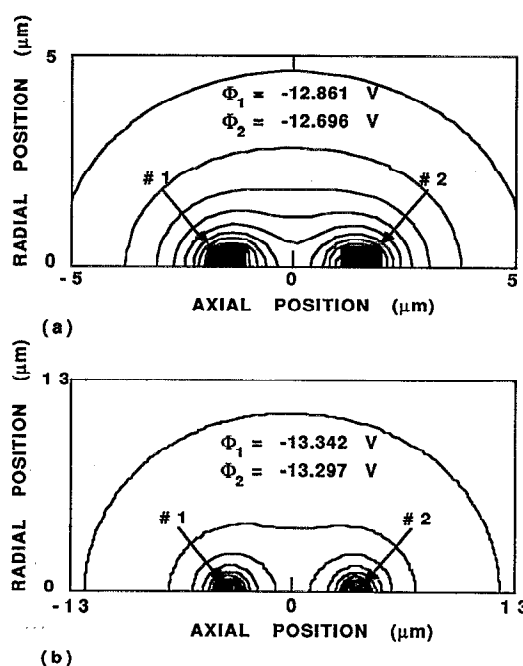
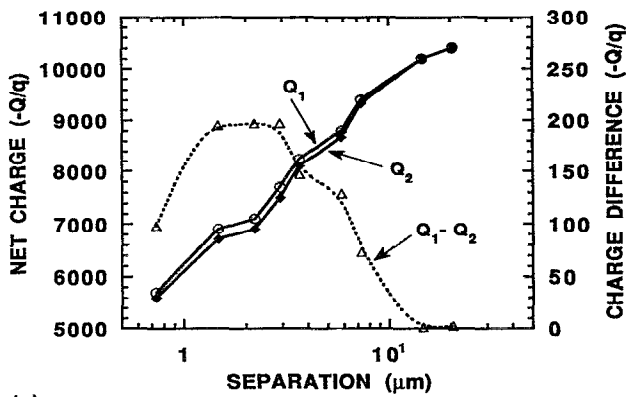


FIG. 1. Plasma potentials around two adjacent identical particles ($d=1 \mu\text{m}$ and $h=0.9 \mu\text{m}$) for separations of (a) 2.2 and (b) $7.3 \mu\text{m}$. The plasma conditions are 0.2 Torr Ar, $3 \times 10^{11} \text{ cm}^{-3}$ bulk plasma density, and 3.9 eV electron temperature. The potentials Φ are noted for each particle. The downstream particle charges less negatively because it is shadowed by the upstream particle.

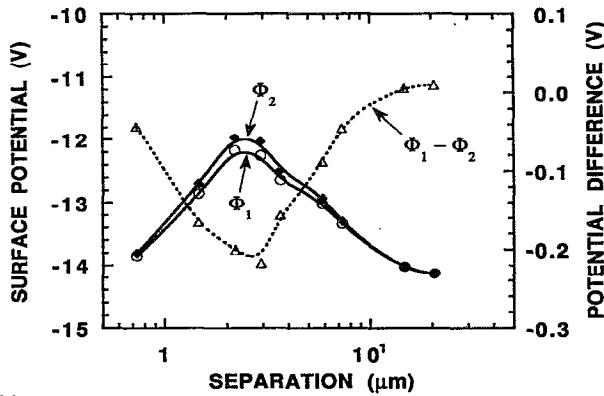
Goertz obtained similar potentials for assemblies of one-dimensional dust grain sheets.²⁷ He also noted that when the spacing between dust grain sheets is less than the Debye length the average charge density on each sheet is reduced due to mutual shielding.

The charge Q (in units of 1.6×10^{-19} coulomb) and potential Φ on the dust particles are shown in Fig. 2 as a function of separation distance. Both particles have a diameter of $1 \mu\text{m}$ and height of $0.9 \mu\text{m}$. The charge and potential on a dust particle are determined by the requirement that the time averaged flux of electrons and ions to its surface are equal. The negative charge, resulting from collection of excess electron current, results in a particle potential of $\approx 1.5 - 3T_e$, somewhat less than the floating potential due to orbiting ion effects.

For our simulation conditions, the charge on an isolated dust particle is $Q/q \approx 10\,500$, corresponding to $\Phi = -14.2 \text{ V}$. As the particles move closer together, the charge on either particle decreases and the potential on either particle increases (to less negative values). As the shielding volumes of the individual particles overlap, the approaching particle contributes to the repulsion of electrons directed towards its neighbor, thereby requiring a smaller potential on its neighbor to maintain a flux balance between electrons and ions. The neighboring particle also intercepts higher energy electrons that would have impacted on the particle. When the particles approach to distances on the order of their size, they begin to resemble a single particle. Their potentials then equilibrate to those for an isolated particle. The sum of the charge on the two



(a)



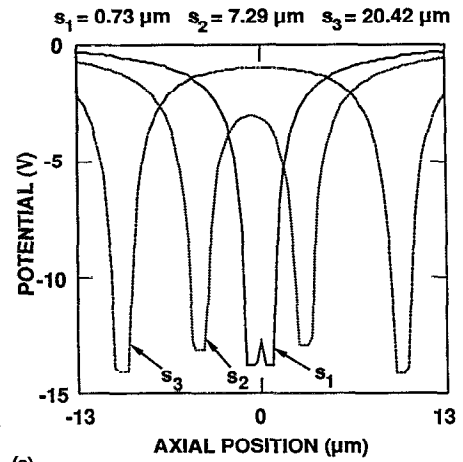
(b)

FIG. 2. Particle charge and potential as a function of separation distance between the particles. (a) Net charges and (b) surface potentials. The conditions are otherwise the same as in Fig. 1.

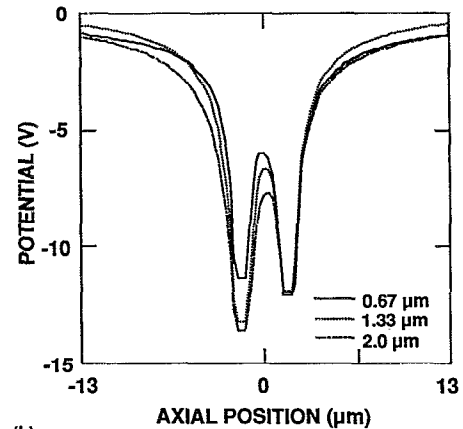
particles is then approximately the same as a single isolated particle.

We observe an interesting shadowing phenomenon that causes the dust particles to have unequal charges when they are aligned parallel to the applied electric field. The upstream particle (with respect to the direction electron drift in the applied field) intercepts a larger electron flux than its neighbor, thereby shadowing the rear particle. As a result, the upstream particle has a more negative surface potential. This shadowing effect is evident in Figs. 1 and 2, in which particle no. 1 is the upstream particle. At large separations, the charge and potential are the same on both particles. As the particles approach the upstream particle charges more negatively and shadows the downstream particle. When the direction of the electric field is reversed, the charge on the particles reverse as the former downstream particle shadows its partner.

The electrical potential is shown in Fig. 3 as a function of axial position ($r=0$) for different particle positions and sizes. In Fig. 3(a), the electrical potentials are shown around two identical dust particles ($d=1 \mu\text{m}$, $h=0.9 \mu\text{m}$) for different separation distances. When two particles are very close to each other, they appear like a single particle due to the nearly complete overlap of their shielding volumes. The slight asymmetry in potential due to shadowing can be seen in the profile for the s_2 separation. The poten-



(a)



(b)

FIG. 3. Electrical potential as a function of axial position ($r=0$) for different particle (a) separations and (b) diameters. The locations of the particles are shown at the top of the lower figure.

tials for particles having different diameters at a fixed separation of $2.9 \mu\text{m}$ are shown in Fig. 3(b). Particles are shown for different diameters of the upstream dust particle (no. 1). The size of the downstream dust particle (no. 2) is fixed at the same size as in Fig. 3(a). As the size of particle no. 1 increases, the overlap of the shielding volumes of the individual particles increases and the shadowing of particle no. 2 increases. [The degree of overlapping of the shielding volumes is indicated by the potential at $z=0$. Isolated particles would have $\Phi(z=0)=0$.]

The net surface charges and the corresponding potentials for particles having different diameters at a fixed separation distance are shown in Fig. 4. The conditions and orientations of the particles are same as in Fig. 3(b). As the size of particle no. 1 increases relative to no. 2 its net surface charge becomes more negative as does its potential. This behavior is to be expected since ions near large particles have less orbital motion. The potential of large particles then begins to resemble floating surfaces and approaches the floating potential. As particle no. 1 increases in size, the amount of negative charge on particle no. 2 decreases slightly, and the surface potential increases to more positive values. The increase in potential results from

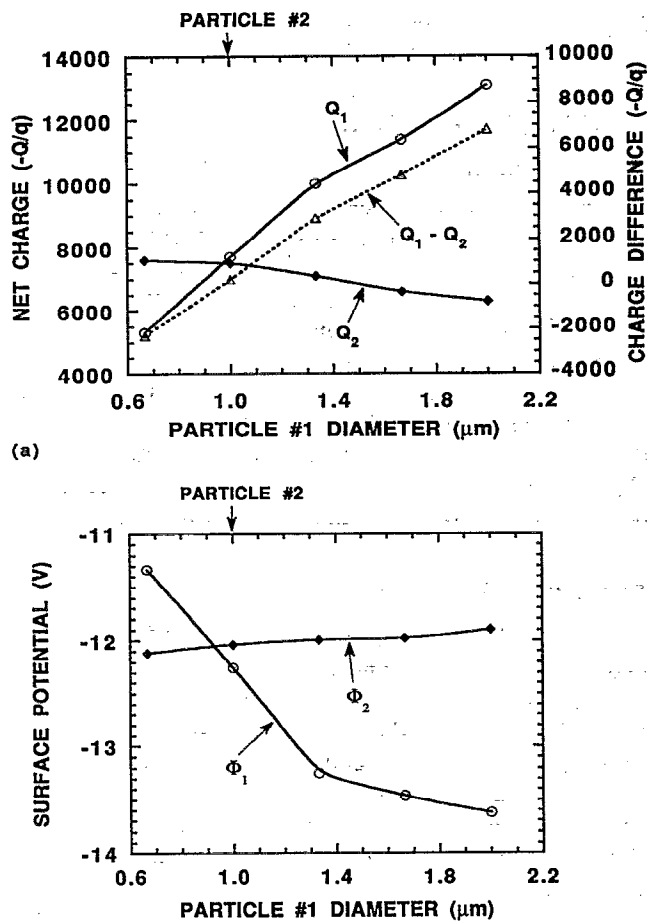


FIG. 4. Net surface charge and surface potential as a function of the diameter of particle no. 1. (a) Net charges on the particles and (b) surface potential of the particles. The size of particle no. 2 is held constant and is shown at the top of each figure.

more effective shadowing of particle no. 2 caused by the increase in the size of particle no. 1.

The shielding of two identical particles ($d=1 \mu\text{m}$, $h=0.9 \mu\text{m}$, separation $2.9 \mu\text{m}$) which are perfect dielectrics was also simulated to examine the local distribution of charges on the surface of the dust particles. The surface charge distributions are shown in Fig. 5. The corresponding potentials are shown in Fig. 6. The upstream dust particle (no. 1) collects total net charge of $-7039/q$ while the downstream dust particle (no. 2) collects total charge of $-6894/q$. The local charge density is highest at the leading edge of particle no. 1 facing upstream. This peak may be due to the collection of the drifting electrons which are diverging away from the negatively charged face. The (absolute) charge density is lowest on the rear face of particle no. 1 and the front face of particle no. 2 because of shadowing which reduces their solid angle view of the bulk plasma. The rear of particle no. 2 has a low charge density because it is in the wake of the drifting electron flux. To some degree, the charge distribution on the dielectric particles suffers from poor statistics. The number of charges on the dust particle is sufficiently small so that there is a component of memory of previously collected electrons or

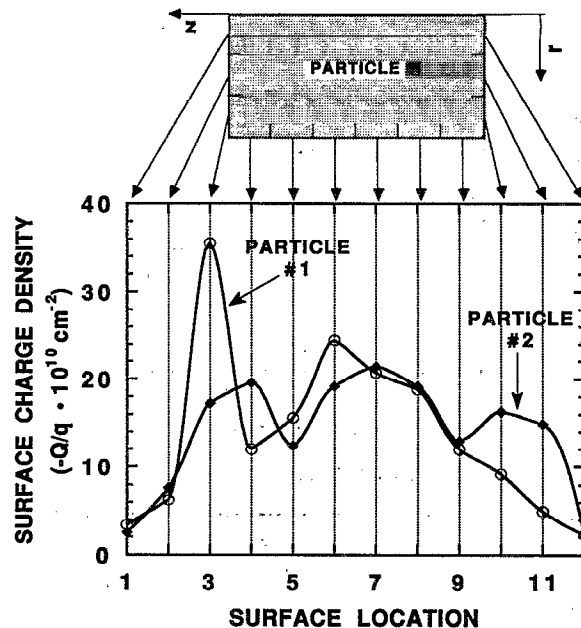


FIG. 5. Surface charge density for perfect dielectric particles. The sizes and conditions are the same as in Fig. 1. The location on the surface is shown by the diagram at the top of the figure. An uneven charge distribution occurs due to shadowing effects.

ions. This statistical noise in the charge distribution causes large field variations near the particles.

Adjacent negatively charged dust particles will, of course, repel each other. Their proximity results from the dominance of other external forces generated by applied potentials, fluid drag, ion drag, or thermophoresis. From our previous calculations,²⁸ we find that in typical plasma processing discharges a $1 \mu\text{m}$ particle could gain kinetic energies on the order of 6×10^{-9} ergs from these forces, or $\approx 4 \text{ keV}$, which is much larger than the intraparticle potentials. Therefore, it is possible for energetic dust particles originating from different locations to move very close to each other and overlap their shielding volumes in spite of their repulsion. Two particles with sufficient kinetic energies can even have contact and produce a particle aggregate.

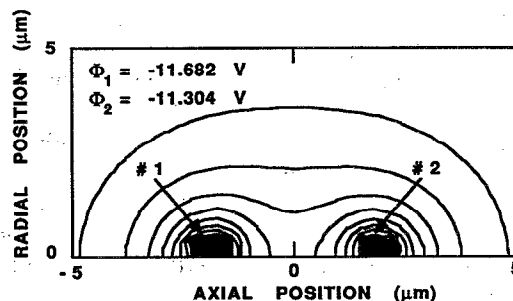


FIG. 6. Plasma potential around the dielectric particles shown in Fig. 5. The equipotential surfaces show some roughness due to the uneven surface charge distribution.

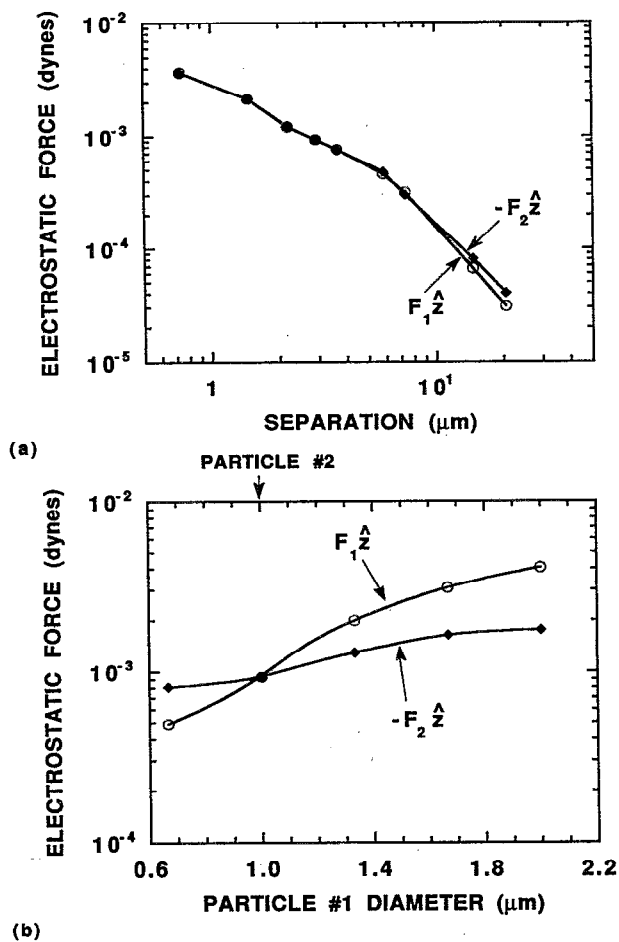


FIG. 7. Electrostatic forces on dual particles as a function of (a) separation distance and (b) size of particle no. 1.

The electrostatic forces on the two adjacent dust particles are shown in Fig. 7 as a function of separation distance and particle size. The electrostatic force is the sum of forces resulting from surface charges, space charges, and externally applied potentials. As expected, at small separation, the magnitude of the forces are equal and opposite, with the vast majority of the force being composed of mutual repulsion. As such, the force on each dust particle decreases almost linearly (on the log plot) with increasing separation distance as shown in Fig. 7(a). The deviation from linearity (on the log plot), as would be expected for pure Coulomb forces, results from the shielding of the particles at large separation. The forces shown in Fig. 7(a) are well represented by the Debye-Hückle form $[Q_1 Q_2 \exp(-r/\lambda_D)/r^2]$. There is also a deviation in the force resulting from the perturbation of the charge distribution between the coupled dust particles and the shadowing effect. At a large separation distance when the mutual shielding is very small, the magnitudes of the forces on the dust particles are slightly different due to the contribution of the applied electric field which reduces the net force on particle no. 1 (upstream particle) and increases the net force on particle no. 2. Figure 7(b) shows the electrostatic forces on the dust particles at a fixed separation distance of

2.9 μm when the size of particle no. 1 varies. The electrostatic force tracks the particle potentials shown in Fig. 4.

IV. CONCLUDING REMARKS

A pseudoparticle-in-cell simulation has been developed and used to investigate the mutual shielding properties of closely spaced dust particles in low temperature plasmas. We found that shadowing of the electron flux occurs when two dust particles are aligned with the electric field. The shadowing consists of the upstream particle intercepting more electron flux, and charging to a more negative potential. The shadowing effect increases as the size of the upstream particle increases because the electron current to the rear dust particle is further obscured. The sum of the charges on the dust particles decrease as their separation decrease and mutual shielding becomes more effective.

ACKNOWLEDGMENTS

The authors would like to thank M. Barnes, A. Garscadden, J. Goree, and D. Graves for their advice and discussions on dusty plasmas. In particular, we thank J. Keller for suggesting that we employ a string of cylindrical dust particles in the simulation. This work was supported by the National Science Foundation (CTS 91-13215 and ECS 91-09326), Sandia National Laboratory, the IBM East Fishkill Facility, and the Semiconductor Research Corporation.

- ¹J. E. Daugherty, R. K. Porteous, M. D. Kilgore, and D. B. Graves, *J. Appl. Phys.* **72**, 3934 (1992).
- ²S. J. Choi and M. J. Kushner, *Appl. Phys. Lett.* **62**, 2197 (1993).
- ³R. M. Roth, K. G. Spears, G. D. Stein, and G. Wong, *Appl. Phys. Lett.* **46**, 235 (1985).
- ⁴G. S. Selwyn, J. E. Heidenreich, and K. L. Haller, *Appl. Phys. Lett.* **57**, 1876 (1990).
- ⁵G. S. Selwyn, J. Singh, and R. S. Bennett, *J. Vac. Sci. Technol. A* **7**, 2758 (1989).
- ⁶G. S. Selwyn, J. S. Mckillop, K. L. Haller, and J. J. Wu, *J. Vac. Sci. Technol. A* **8**, 1726 (1990).
- ⁷G. M. Jellum and D. B. Graves, *Appl. Phys. Lett.* **57**, 2077 (1990).
- ⁸G. M. Jellum and D. B. Graves, *J. Appl. Phys.* **67**, 6490 (1990).
- ⁹G. M. Jellum, J. E. Daugherty, and D. B. Graves, *J. Appl. Phys.* **69**, 6923 (1991).
- ¹⁰Y. Watanabe, M. Shiratani, and H. Makino, *Appl. Phys. Lett.* **57**, 1616 (1990).
- ¹¹Y. Watanabe, M. Shiratani, and M. Yamashita, *Appl. Phys. Lett.* **61**, 1510 (1992).
- ¹²R. N. Carlile, S. G. Geha, J. O'Hanlon, and J. Stewart, *Appl. Phys. Lett.* **59**, 1167 (1991).
- ¹³T. J. Sommerer, M. S. Barnes, J. H. Keller, M. J. McCaughey, and M. J. Kushner, *Appl. Phys. Lett.* **59**, 638 (1991).
- ¹⁴M. S. Barnes, J. H. Keller, J. C. Forster, J. A. O'Neill, and D. K. Coultas, *Phys. Rev. Lett.* **68**, 313 (1992).
- ¹⁵S. G. Geha, R. N. Carlile, J. F. O'Hanlon, and G. S. Selwyn, *J. Appl. Phys.* **72**, 374 (1992).
- ¹⁶L. Boufendi, A. Bouchoule, R. K. Porteous, J. Ph. Blondeau, A. Plain, and C. Laure, *J. Appl. Phys.* **73**, 2160 (1993).
- ¹⁷J. Goree and T. E. Sheridan, *J. Vac. Sci. Etch. A* **10**, 3540 (1992).
- ¹⁸K. R. Stalder, *Proc. SPIE* **1185**, 164 (1989).
- ¹⁹S. J. Choi and M. J. Kushner, "A Particle-in-Cell Simulation of Dust Charging and Shielding in Low Pressure Glow Discharges," *Trans. Plasma Sci.* (to be published).
- ²⁰J. S. Logan and J. J. McGill, *J. Vac. Sci. Technol. A* **10**, 1875 (1992).
- ²¹M. D. Kilgore, J. E. Daugherty, R. K. Porteous, and D. B. Graves, *J. Vac. Sci. Technol. B* (to be published).

²²Y. Weng and M. J. Kushner, *Phys. Rev. A* **42**, 6192 (1992).

²³A. V. Phelps, *J. Phys. Chem. Ref. Data* **21**, 883 (1992).

²⁴A. V. Phelps, *J. Phys. Chem. Ref. Data* **20**, 557 (1991).

²⁵J. Hopwood, *Plasma Sources Sci. Technol.* **1**, 109 (1992).

²⁶The linearized Debye length characterizes the shielding of dust particles in plasmas: $\lambda_L = [(q^2 n / \epsilon_0) (1/kT_e + 1/2E_+)]^{-1}$, where n is the ion den-

sity, T_e is the electron temperature, and E is the ion energy. See Ref. 1.

²⁷C. K. Goertz, *Rev. Geophys.* **27**, 271 (1989).

²⁸S. J. Choi, P. L. G. Ventzek, R. J. Hoekstra, and M. J. Kushner, "Spatial Distributions of Dust Particles in Plasmas Generated by Capacitively Coupled Radio Frequency Discharges," *Plasma Sources Sci. Technol.* (to be published).